Investigation of a Tetrathiafulvalene-Based Fe²⁺ Thermal Spin Crossover Assembled on Gold Surface

Niccolò Giaconi [1,2], **Andrea Luigi Sorrentino** [1,2], **Lorenzo Poggini** [3,*], **Giulia Serrano** [1,2], **Giuseppe Cucinotta** [1], **Edwige Otero** [4], **Danilo Longo** [4], **Haiet Douib** [5], **Fabrice Pointillart** [5], **Andrea Caneschi** [2], **Roberta Sessoli** [1] and **Matteo Mannini** [1,*]

[1] Department of Chemistry "U. Schiff"-DICUS and INSTM Research Unit, University of Florence, Via della Lastruccia 3-13, Sesto Fiorentino, 50019 Florence, Italy; niccolo.giaconi@unifi.it (N.G.); andrealuigi.sorrentino@unifi.it (A.L.S.); giulia.serrano@unifi.it (G.S.); giuseppe.cucinotta@unifi.it (G.C.); roberta.sessoli@unifi.it (R.S.)

[2] Department of Industrial Engineering-DIEF and INSTM Research Unit, University of Florence, Via Santa Marta 3, 50139 Florence, Italy; andrea.caneschi@unifi.it

[3] Institute for Chemistry of OrganoMetallic Compounds (ICCOM-CNR), Via Madonna del Piano, Sesto Fiorentino, 50019 Florence, Italy

[4] Synchrotron SOLEIL, L'Orme des Merisiers, CEDEX 48, 91192 Gif-sur-Yvette, France; edwige.otero@synchrotron-soleil.fr (E.O.); d.longo@nanogune.eu (D.L.)

[5] ISCR (Institut des Sciences Chimiques de Rennes)—UMR 6226, CNRS, University of Rennes, 35042 Rennes, France; haiet.douib@univ-rennes1.fr (H.D.); fabrice.pointillart@univ-rennes1.fr (F.P.)

* Correspondence: lpoggini@iccom.cnr.it (L.P.); matteo.mannini@unifi.it (M.M.)

Abstract: A thick film and a monolayer of tetrathiafulvalene-based Fe²⁺ spin-crossover complex have been deposited by solution on a Au (111) substrate, attempting both self-assembling monolayer protocol and a simpler drop-casting procedure. The thermally induced spin transition has been investigated using X-ray photoelectron spectroscopy (XPS) and X-ray absorption spectroscopy (XAS). Temperature-dependent investigations demonstrated the retention of the switching behavior between the two spin states in thick molecular films obtained by drop-casting, while in the monolayer sample, the loss of the spin-crossover properties appears as a possible consequence of the strong interaction between the sulfur atoms of the ligand and the gold substrate.

Keywords: tetrathiafulvalene; iron (II); spin-crossover; XPS; XAS; molecular film

1. Introduction

Spin-crossover (SCO) compounds [1] are complexes of metal ions capable of switching between two spin states after the application of several kinds of external stimuli, such as temperature, pressure, magnetic or electric field, and light irradiation [2–6]. The reversible switching between the two spin states is accompanied by relevant changes in the chemical, physical, optical, and magnetic properties of molecules, and it makes these complexes very attractive for a wide range of applications [7,8]. In the case of Fe²⁺ complexes with octahedral geometry, this transition involves electrons in *3d* orbitals that can be arranged in a low-spin (LS) state configuration with $S = 0$ or in a high-spin (HS) state configuration with $S = 2$, thus moving from a diamagnetic system to a paramagnetic one and vice versa [9]. Being that SCO complexes very interesting as building blocks for the development of molecular-based spintronics devices [10,11], the nanostructuration of these molecules on the surface represents a fundamental step. In recent decades, SCO behavior has been reported in several complexes deposited on surfaces as thick and thin films, mainly obtained by thermal sublimation protocols [12]. However, the persistence of SCO behavior in (sub)monolayer deposits [13,14] suffers from several limitations that complicate the perspective of the development of an SCO-based technology. In particular, it has been observed that strong modifications or losses in the spin switching properties can occur once

molecules are assembled on a surface due to a strong interaction with the substrate, as well as to the role played by intermolecular interactions [15–17]. This is particularly relevant when pristine molecules are directly in contact with metallic surfaces [18] and minimized when specific surfaces are selected [19,20]. The alternative approach of separating the SCO active unit from the surface is represented by a chemical approach based on the chemisorption of functionalized SCO units on the surface; however, up to now, we still lack a clear demonstration of the persistence of a spin transition in a chemically anchored monolayer deposit.

In this work, we studied the mononuclear Fe^{2+} SCO complex [Fe(H_2Bpz$_2$)$_2$(**L**)] (H_2Bpz$_2$ = dihydrobis(1-pyrazolyl)-borate) where **L**= TTF (tetrathiafulvalene)-fused dipyrido-[*3,2-a:2′,3′-c*] phenazine (dppz) ligand (Figure 1a). This complex has been previously synthesized and studied by some of us observing the occurrence of a thermal spin-crossover around 143 K with a pronounced hysteresis behavior (48 K) [21]. Here, this system has been investigated, probing the feasibility of anchoring a monolayer of these molecules on the surface, profiting from the interaction between two thioether groups and the gold surface that was expected to promote either chemisorption with the homolytic C-S bond cleavage or just physisorption. In addition, the ligand **L** may play the role of a spacer between the iron center and the metallic surface. The molecular monolayer was obtained by adopting a standard self-assembling monolayer (SAM) deposition protocol and was confirmed spectroscopically using the edge jump method from XAS [22]. In parallel, thick films were produced via *drop-casting*. Both deposits were characterized with spectroscopic techniques, such as X-ray photoelectron spectroscopy (XPS) and X-ray absorption spectroscopy (XAS), deputed to follow the SCO phenomenon [23]. In the monolayer deposit, due to a modification of the structure of the complex, the switching behavior was not clearly detected, while, in the thicker film, the SCO behavior was observed, despite the occurrence of some variations attributable to a modification of the crystal packing.
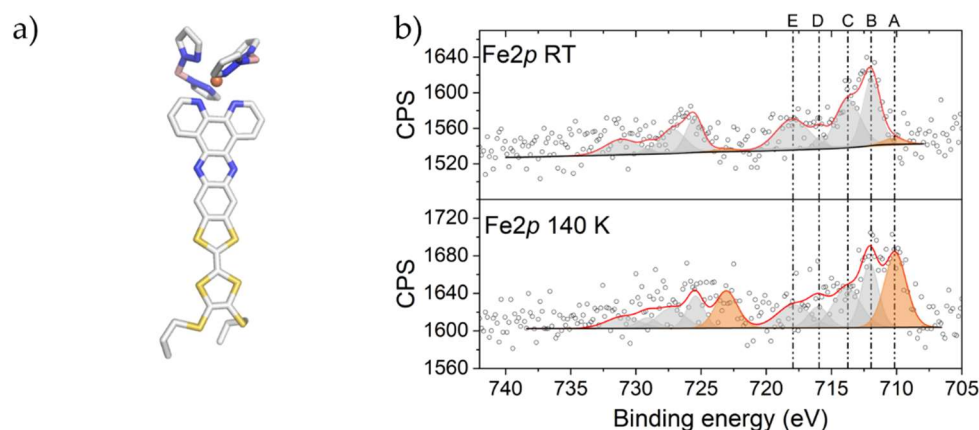
Figure 1. (**a**) X-ray molecular structure of [Fe(H_2Bpz$_2$)$_2$(**L**)]. Sulfur, yellow; nitrogen, blue; carbon, light grey; iron, orange; boron, pink. (**b**) Fe2*p* region XPS spectra of [Fe(H_2Bpz$_2$)$_2$(**L**)] thick film on Au acquired at RT (top) and 140 K (bottom). Orange components, attributable to LS species, show a temperature dependence, evidencing the SCO behavior of the complex. (See Table S1 for further details).

2. Results and Discussion

2.1. X-ray Photoelectron Spectroscopy (XPS) Characterization

The XPS technique was used to fully characterize the chemical- and temperature-dependent electronic properties of the thin and thick films of [Fe(H_2Bpz$_2$)$_2$(**L**)] (the molecular X-ray structure is reported in Figure 1a). XPS was fundamental in evaluating the chemical integrity of this system after the deposition processes; moreover, experiments were repeated at both RT and 140 K to evidence, by monitoring the spectral shape in the Fe2*p* region of interest, the occurrence of a spin-crossing over [3,11,24].

First, a thick film, obtained by *drop-casting,* was investigated. Being the thickness of the deposit of the order of hundreds of nanometers, and given the scarce penetration depth of the photoelectrons, we can exclude in this sample the occurrence of a significant interaction between the molecules and the Au surface in the sampled region. This is confirmed by the observation (see Supplementary Materials, Figure S1a) of a single feature in the S2p region, which is actually given by the overlap between the S2$p_{3/2}$ and the S2$p_{1/2}$ contributions found at 162.8 eV and 164 eV respectively, and attributable to the sulfur atoms of the TTF moiety of the ligand [3]. The absence of components at a lower binding energy (ca. 161–161.5 eV) confirms that a chemical bond between the sulfur and gold atoms on the surface is not present [3].

Figure 1b reports the analysis in the Fe2p region of the thick film at RT and 140 K. The deconvolution analysis of both reported iron spectra agrees with previous literature reports for Fe^{2+} in an octahedral geometry, and the variation in the spectral fine structure is in line with the partial conversion from the HS- and LS-state configuration obtained by decreasing the temperature [11,24,25].

Indeed, the thermally driven SCO behavior is confirmed by the temperature dependence of the line shape of the spectra, where a relevant variation in the component at 710.1 eV (Figure 1b), the one attributable to Fe^{2+} LS, is observed [26]. Additionally, the presence of a second main peak at ca. 711.9 eV is attributable to the multiplets splitting that is expected for XPS 2p spectra of an iron species [26,27]. Further confirmation of the occurring thermal transition is given by evaluating the spin-orbit splitting (Δ_{SO}) between the Fe2$p_{3/2}$ and Fe2$p_{1/2}$ extracted components, with Δ_{SO} being lower for the LS state than for the HS state due to a different orbital population which does not involve e_g-like orbitals when the system exists in the LS state. Table S1 reports the Δ_{SO} evaluated from the different components used for the deconvolution analysis reported in Figure 1b; these values are in good agreement with those previously reported in the literature [28]. Satellite spectral features occurring at higher binding energy (see Table S1 in the Supplementary Materials) are characteristic of a two-hole bound state induced by the photoemission and the resulting excitation from the Highest Occupied Molecular Orbital (HOMO) to the unoccupied states [25,29]. The analysis of the N1s region suggests the presence of one component at 398.9 eV, attributable to the nitrogen atoms of the H$_2$Bpz$_2$ ligand [30], as reported in Figure S1b, while the C1s main component (Figure S1c) was used to calibrate the spectra and was set to 284.5 eV, being attributed to the aliphatic and aromatic carbon atoms and the adventitious carbon species [31]. Two additional components were included to properly reproduce the experimental C1s spectra: one component assigned to C-S/C-N (285.9 eV) [11,24], and the second was attributed to carboxylic groups that might come from environmental contamination (288.6 eV) [32]. A semi-quantitative analysis was performed, taking into account the Fe2p, S2p, and N1s signals. The C1s signal was not considered because of potential adventitious contamination. Considering the experimental error of the XPS, the measured percentages for the drop-cast sample are comparable with theoretical values (Table S2). Furthermore, analyzing the ratio between areas of the components of Fe2p regions, a quantitative estimation of the HS percentage was extracted from the Fe2p region, passing from 96.4% at room temperature to 67.5% at 140 K.

From the analogue characterization performed on the monolayer deposit, clearly comes out that the interaction between the sulphur atoms and the gold substrate is so strong that S-Au bonds occur between the terminal sulphur atoms as well as with sulphur belonging to the TFF ring (Figure S2) because the expected ratio between the component at 163.8 eV (physisorbed) and the one at 161.5 eV (chemisorbed) should be 2:1, at variance we have found a ratio of 1.4, revealing the occurrence of more S-Au bonds than expected. This interaction induces a change in the chemical structure of the compound (see Table S2) compared to the bulk phase. An attempt has been made to quantitatively analyse the molecular film trying to estimate the stoichiometry of the molecules after the monolayer assembly. However, we assume that, due to the very low intensity of the signals, the results obtained are not reliable. In addition, the Fe2p region spectra acquired on the monolayer

sample do not show any relevant variation of the line shape as a function of temperature (Figure S3) from RT to 140 K. Given the small number of molecules assembled on the surface close to the limit of the sensitivity of our XPS setup, and given the limited range of temperatures that we can probe, the slight variation in the Fe$2p$ XPS line shape as a function of the temperature is not conclusive about the retention or absence of the SCO properties that must be investigated with a more sensitive characterization technique, such as XAS, exploiting the synchrotron radiation.

2.2. X-ray Absorption Spectroscopy (XAS) Characterization

X-ray absorption spectroscopy (XAS) was employed to investigate the thermal-induced SCO behavior of [Fe(H$_2$Bpz$_2$)$_2$(**L**)], both on the monolayer and on the bulk/thick film. Performing XAS at the Fe L$_{2,3}$ edge gives us information about the transition of electrons excited from 2p orbitals to 3d orbitals, which are directly involved in the thermal spin-crossover transition. Indeed, in the LS state, the three t_{2g} orbitals are fully occupied, leaving the e_g orbitals empty. In HS state, also e_g orbitals are partially filled with two unpaired electrons. These thermally induced mechanics can be followed by observing the variation in the line shape of the XAS spectra [23,33–35].

On the thick film, the XAS Fe L$_{2,3}$ temperature dependence was detected, as reported in Figure 2a. The complete XAS spectra series acquired at the Fe L$_{2,3}$ edge from 70 K up to RT (warming mode) is reported in Figure S4. Differing from what was observed in the crystalline bulk phase by magnetometry measurements [21], at T < 195 K, a complete conversion to the LS state does not occur. We suggest that the incomplete LS-state conversion of the system could be attributed to a change in the intermolecular interaction after the deposition process. Indeed, it is well known that the cooperativity effect plays a crucial role in the SCO phenomenon [36].
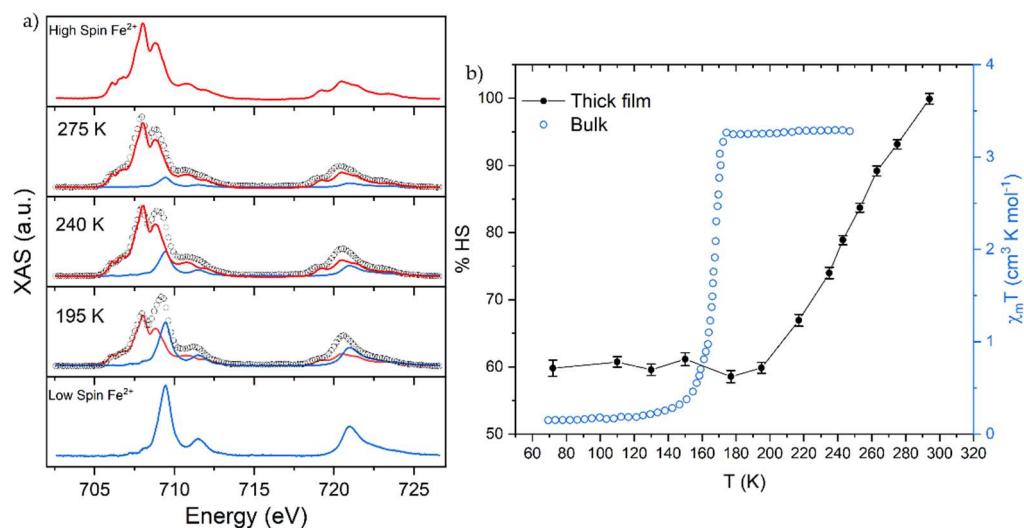
Figure 2. (**a**) Temperature dependence of normalized, experimental Fe L$_{2,3}$ edge XAS spectra of [Fe(H$_2$Bpz$_2$)$_2$(**L**)] thick film (empty dots) with contribution of high-spin Fe^{2+} (red line) and low-spin Fe^{2+} (blue line). [Fe(H$_2$B(pz)$_2$)$_2$(2,2$'$-bipy)] XAS spectra are taken as HS and LS references. Reprinted from Ref. [37]. (**b**) High-spin Fe^{2+} percentage distribution as a function of temperature (black dots) and magnetic susceptibility characterization of powder of [Fe(H$_2$Bpz$_2$)$_2$(**L**)]. Reprinted from Ref. [21].

Even at 70 K (Figure S4), both components (LS and HS) are necessary to properly reproduce the experimental data, confirming the coexistence of both species until 275 K. As shown in Figure 2b, where an estimation of HS species as a function of temperature is reported, a fraction of the HS state is also present at a low temperature with a percentage of ca. 60%, in line with the percentage found in the crystalline bulk system. When the temperature was increased, a change in the shape of the spectra could be observed together

with an enhancement of the HS state of up to 100% at room temperature. Furthermore, unlike the powder characterization of [Fe(H$_2$Bpz$_2$)$_2$(**L**)], where an abrupt transition at T$_{1/2}$=167 K in warming mode was detected, here, a gradual, thermally induced transition with a T$_{1/2}$ = 243 K was observed. This variation can be ascribed to the drop-cast deposition process, as already reported in the past, for instance, by Cini et al. [15] for a similar Fe^{2+} SCO complex. Indeed, similar to what we detected in this system, it was observed that a strong difference, both in the percentage of spin conversion and in T$_{1/2}$ value between the powder and the thick film, can occur because of changes in the intermolecular interaction as well as in the distortion of the molecule with respect to the regular structure assumed in the crystal. Furthermore, differences in the SCO switching behaviour could also be due to the characterization technique exploited to probe the transition. Indeed, as demonstrated by Zhang et al. [23], spectroscopic techniques such as XAS leave the investigated system in an out-of-equilibrium state that is associated with a change in several parameters of the complex, such as sample conductance, crystal packing, or steric hindrance. Modification of these properties is not negligible in determining the transition temperature. Indeed, in several Fe^{2+} spin-crossover complexes, a relevant deviation of T$_{1/2}$ probed with XAS, compared to the one measured with magnetometry, has been observed.

The same characterization, monitoring the temperature dependence of the spectra, was carried out on the SAM sample, but, unfortunately, we observed a complete loss of the SCO behaviour, as already observed by XPS measures. We suggest that a higher number of S-Au bonds per molecule than the expected two at the thiopropyl moieties could induce not only a change in the chemical structure of the complex, but also a lying configuration of the molecule on the surface, thus approaching the iron centre to the substrate [38]. This loss of SCO behaviour can be seen in Figure S5, where XAS spectra at RT and 80 K are reported; no variation in the XAS line shape can be detected, and both spectra clearly indicate the presence of Fe^{3+} [39] on the surface. The latter evidence confirms that the molecular structure of [Fe(H$_2$Bpz$_2$)$_2$(**L**)] undergoes degradation [40] during the deposition on the gold surface here tested, and it excludes the possibility that this protocol can be used to achieve an intact monolayer of [Fe(H$_2$Bpz$_2$)$_2$(**L**)].

3. Materials and Methods

The [Fe(H$_2$Bpz$_2$)$_2$(**L**)] complex was synthesized by following the procedure already reported in the literature [21]. The substrate was prepared by evaporating gold (110 nm) on a freshly cleaved mica substrate inside a vacuum chamber (ca. 10^{-7} mbar) with a deposition rate lower than 0.1 Å/s. The substrate was annealed with an H$_2$ flame to induce the reconstruction of a Au(111) surface [41]. The molecular monolayer was deposited by incubating the substrate in a 2 mM solution of [Fe(H$_2$Bpz$_2$)$_2$(**L**)] in CH$_2$Cl$_2$ for 24 h at room temperature with the aim of inducing a densely packed SAM. Thus, the surface was rinsed first with pure CH$_2$Cl$_2$, then with pure CHCl$_3$, and dried under N$_2$ atmosphere. In parallel, a thick film deposit was obtained by drop-casting a few drops of the same solution on a gold substrate and then removing the solvent using a N$_2$ flux, leaving a thick and non-homogeneous deposit of molecules on the surface as an amorphous film of a few hundred nanometres thick. The sample was heated up to facilitate the removal of the solvent; indeed, the presence of residual solvent molecules in the crystal may quench the thermal SCO transition. The absence of dichloromethane molecules was further confirmed investigating the Cl2*p* XPS region where any signals was not detected (Figure S1d).

XPS measurements were performed using a micro-focused, monochromatic Al K$_\alpha$ radiation source (1486.6 eV, model SPECS XR-MS Focus 600) and a multichannel-detector electron analyzer (model SPECS Phoibos 150 1DLD) with a pass energy of 40 eV to ensure appropriate resolution. The spectra were measured in normal emission, with the X-ray source mounted at 54.44° from the analyser. The binding energy was calibrated using the C1*s* peak at 284.5 eV. Spectra were deconvoluted using CasaXPS software, introducing mixed Gaussian and Lorentzian contributions for each component. The background was fitted using the Shirley or linear baseline.

The XAS experiments were performed at the DEIMOS beamline [42] using the SOLEIL synchrotron. The spectra were acquired in reduced photon-flux conditions to prevent any radiation damage to the sample, and the signal was acquired in total electron yield (TEY) [43] detection mode. The XAS spectra were acquired at the Fe $L_{2,3}$ edges using right-circular polarized light at a normal incidence ($\theta = 0°$), where θ was defined as the angle between the *k* X-ray propagation vector and the normal n to the surface, which always lies in the horizontal plane. The temperature dependence of the HS and the LS-Fe^{2+} fractions was estimated through least-squares interpolation of normalized XAS spectra by using two references of a similar octahedral spin-crossover Fe^{2+} complex (both in a chemical environment and $T_{1/2}$), recorded at 100 K and 300 K where, respectively, a 100% contribution of these configurations is expected [37].

4. Conclusions

In summary, we studied the SCO behaviour of an Fe^{2+} TTF-based ligand complex, both of a bulky deposit and as a monolayer, exploiting two X-ray spectroscopic techniques, XPS and XAS, aiming to observe the thermally induced spin transition. Due to the strong interaction between the ligand and the gold substrate, we observed the loss of the SCO properties in the monolayer sample, accompanied by chemical structure changes after the deposition process. However, in the thicker sample, we were able to observe, either by XPS or XAS, a spin transition of the molecular film as a function of the temperature, although with significant changes with respect to the crystalline bulk phase.

Despite the possibility of anchoring [Fe(H_2Bpz$_2$)$_2$(**L**)] on a gold surface by exploiting two S-Pr terminal groups, we revealed that the interaction between the molecules and the surface is so strong that the sulphur atoms of the TTF backbone are also involved in the formation of the S-Au bonds. This modified the structure of the complex, approaching the metal centre to the surface and inducing a quench of the spin-switching properties. However, by slightly increasing the thickness of the molecular film, we detected the retention of the SCO behaviour. This paves the way for the chemical modification of the TTF ligand to avoid the ion–surface interaction, making this system attractive for the development of a molecular-based spintronic device [44].

Supplementary Materials: The following are available online at https://www.mdpi.com/article/10.3390/magnetochemistry8020014/s1: Figure S1: S2*p*, N1*s,* and C1*s* regions of the XPS spectra of [Fe(H_2Bpz$_2$)$_2$(**L**)] thick film on Au; Table S1: Component used for fitting Fe2*p* XPS spectra of [Fe(H_2Bpz$_2$)$_2$(**L**)] thick film on Au; Figure S2: S2*p* region of XPS spectra of [Fe(H_2Bpz$_2$)$_2$(**L**)] monolayer on Au; Table S2: Semi-quantitative analysis of [Fe(H_2Bpz$_2$)$_2$(**L**)] thick film and of [Fe(H_2Bpz$_2$)$_2$(**L**)]@Au(111); and Figure S3: Fe2*p* region of XPS spectra of [Fe(H_2Bpz$_2$)$_2$(**L**)]@Au(111) at room temperature and at 140 K. Figure S4: XAS spectra at the Fe $L_{2,3}$ edge of [Fe(H_2Bpz$_2$)$_2$(**L**)] thick film between 295 K and 70 K. Experimental spectra (dots), HS contribution (red line) and LS contribution (blue line); Figure S5: XAS spectra at the Fe $L_{2,3}$ edge of [Fe(H_2Bpz$_2$)$_2$(**L**)]@Au(111) at 80 K and 295 K.

Author Contributions: Conceptualization, M.M. and L.P.; software, G.C.; synthesis, F.P. and H.D.; XPS investigation, N.G., A.L.S., L.P., G.S., M.M. and A.C.; XAS investigation N.G., A.L.S., L.P., G.S., M.M., G.C., E.O. and D.L.; data curation, N.G., L.P.; writing—original draft preparation, N.G.; writing—review and editing, L.P., M.M., R.S., A.C.; supervision, M.M., L.P.; project administration, M.M.; funding acquisition, R.S., A.C., M.M. All authors have read and agreed to the published version of the manuscript.

Funding: The European COST Action CA15128 MOLSPIN, the European Commission through the ERC-CoG 725184 MULTIPROSMM (project n. 725184), and the FET Open Femtoterabyte project are acknowledged for financial support. Italian MIUR for Progetto Dipartimenti di Eccellenza 2018-2022 project (ref. B96C1700020008) and Fondazione Cassa di Risparmio di Firenze for SPIN-E2 project (ref. 2020.1634) are also acknowledged for financial support.

Data Availability Statement: The data presented in this study are available on request from the corresponding authors.

Acknowledgments: We acknowledge SOLEIL for the provision of synchrotron radiation facilities. We thank P. Ohresser and L. Joly for their assistance in using the DEIMOS beamline (proposal 20191797).

Conflicts of Interest: The authors declare no conflict of interest.

References

1. Gütlich, P.; Goodwin, H.A. Spin Crossover—An Overall Perspective. In *Spin Crossover in Transition Metal Compounds I*; Springer: Berlin/Heidelberg, Germany, 2004; pp. 1–47. [CrossRef]
2. Poggini, L.; Gonidec, M.; Canjeevaram Balasubramanyam, R.K.; Squillantini, L.; Pecastaings, G.; Caneschi, A.; Rosa, P. Temperature-induced transport changes in molecular junctions based on a spin crossover complex. *J. Mater. Chem. C* **2019**, *7*, 5343–5347. [CrossRef]
3. Poggini, L.; Londi, G.; Milek, M.; Naim, A.; Lanzilotto, V.; Cortigiani, B.; Bondino, F.; Magnano, E.; Otero, E.; Sainctavit, P.; et al. Surface effects on a photochromic spin-crossover iron(II) molecular switch adsorbed on highly oriented pyrolytic graphite. *Nanoscale* **2019**, *11*, 20006–20014. [CrossRef]
4. Poggini, L.; Milek, M.; Londi, G.; Naim, A.; Poneti, G.; Squillantini, L.; Magnani, A.; Totti, F.; Rosa, P.; Khusniyarov, M.M.; et al. Room temperature control of spin states in a thin film of a photochromic iron(II) complex. *Mater. Horizons* **2018**, *5*, 506–513. [CrossRef]
5. Gutlich, P.; Knenofontov, V.; Gaspar, A. Pressure effect studies on spin crossover systems. *Coord. Chem. Rev.* **2005**, *249*, 1811–1829. [CrossRef]
6. Real, J.A.; Gaspar, A.B.; Muñoz, M.C. Thermal, pressure and light switchable spin-crossover materials. *Dalt. Trans.* **2005**, *12*, 2062. [CrossRef] [PubMed]
7. Senthil Kumar, K.; Ruben, M. Emerging trends in spin crossover (SCO) based functional materials and devices. *Coord. Chem. Rev.* **2017**, *346*, 176–205. [CrossRef]
8. Molnár, G.; Rat, S.; Salmon, L.; Nicolazzi, W.; Bousseksou, A. Spin Crossover Nanomaterials: From Fundamental Concepts to Devices. *Adv. Mater.* **2018**, *30*, 1703862. [CrossRef]
9. Gütlich, P. Spin crossover in iron(II)-complexes. In *Metal Complexes*; Springer: Berlin/Heidelberg, Germany, 1981; pp. 83–195. [CrossRef]
10. Cucinotta, G.; Poggini, L.; Giaconi, N.; Cini, A.; Gonidec, M.; Atzori, M.; Berretti, E.; Lavacchi, A.; Fittipaldi, M.; Chumakov, A.I.; et al. Space Charge-Limited Current Transport Mechanism in Crossbar Junction Embedding Molecular Spin Crossovers. *ACS Appl. Mater. Interfaces* **2020**, *12*, 31696–31705. [CrossRef]
11. Poggini, L.; Gonidec, M.; González-Estefan, J.H.; Pecastaings, G.; Gobaut, B.; Rosa, P. Vertical Tunnel Junction Embedding a Spin Crossover Molecular Film. *Adv. Electron. Mater.* **2018**, *4*, 1800204. [CrossRef]
12. Kumar, K.S.; Ruben, M. Sublimable Spin-Crossover Complexes: From Spin-State Switching to Molecular Devices. *Angew. Chemie Int. Ed.* **2021**, *60*, 7502–7521. [CrossRef]
13. Kelai, M.; Repain, V.; Tauzin, A.; Li, W.; Girard, Y.; Lagoute, J.; Rousset, S.; Otero, E.; Sainctavit, P.; Arrio, M.-A.; et al. Thermal Bistability of an Ultrathin Film of Iron(II) Spin-Crossover Molecules Directly Adsorbed on a Metal Surface. *J. Phys. Chem. Lett.* **2021**, *12*, 6152–6158. [CrossRef] [PubMed]
14. Ossinger, S.; Kipgen, L.; Naggert, H.; Bernien, M.; Britton, A.J.; Nickel, F.; Arruda, L.M.; Kumberg, I.; Engesser, T.A.; Golias, E.; et al. Effect of ligand methylation on the spin-switching properties of surface-supported spin-crossover molecules. *J. Phys. Condens. Matter* **2019**, *32*, 114003. [CrossRef] [PubMed]
15. Cini, A.; Poggini, L.; Chumakov, A.I.; Rüffer, R.; Spina, G.; Wattiaux, A.; Duttine, M.; Gonidec, M.; Fittipaldi, M.; Rosa, P.; et al. Synchrotron-based Mössbauer spectroscopy characterization of sublimated spin crossover molecules. *Phys. Chem. Chem. Phys.* **2020**, *22*, 6626–6637. [CrossRef] [PubMed]
16. Konig, E.; Ritter, G.; Kulshreshtha, S.K. The nature of spin-state transitions in solid complexes of iron(II) and the interpretation of some associated phenomena. *Chem. Rev.* **1985**, *85*, 219–234. [CrossRef]
17. Hauser, A.; Jeftić, J.; Romstedt, H.; Hinek, R.; Spiering, H. Cooperative phenomena and light-induced bistability in iron(II) spin-crossover compounds. *Coord. Chem. Rev.* **1999**, *190–192*, 471–491. [CrossRef]
18. Zhang, L.; Tong, Y.; Kelai, M.; Bellec, A.; Lagoute, J.; Chacon, C.; Girard, Y.; Rousset, S.; Boillot, M.; Rivière, E.; et al. Anomalous Light-Induced Spin-State Switching for Iron(II) Spin-Crossover Molecules in Direct Contact with Metal Surfaces. *Angew. Chemie Int. Ed.* **2020**, *59*, 13341–13346. [CrossRef]
19. Rohlf, S.; Grunwald, J.; Jasper-Toennies, T.; Johannsen, S.; Diekmann, F.; Studniarek, M.; Berndt, R.; Tuczek, F.; Rossnagel, K.; Gruber, M. Influence of Substrate Electronic Properties on the Integrity and Functionality of an Adsorbed Fe(II) Spin-Crossover Compound. *J. Phys. Chem. C* **2019**, *123*, 17774–17780. [CrossRef]
20. Zhang, X.; Costa, P.S.; Hooper, J.; Miller, D.P.; N'Diaye, A.T.; Beniwal, S.; Jiang, X.; Yin, Y.; Rosa, P.; Routaboul, L.; et al. Locking and Unlocking the Molecular Spin Crossover Transition. *Adv. Mater.* **2017**, *29*, 1702257. [CrossRef]
21. Pointillart, F.; Liu, X.; Kepenekian, M.; Le Guennic, B.; Golhen, S.; Dorcet, V.; Roisnel, T.; Cador, O.; You, Z.; Hauser, J.; et al. Thermal and near-infrared light induced spin crossover in a mononuclear iron(II) complex with a tetrathiafulvalene-fused dipyridophenazine ligand. *Dalt. Trans.* **2016**, *45*, 11267–11271. [CrossRef]

22. Totaro, P.; Poggini, L.; Favre, A.; Mannini, M.; Sainctavit, P.; Cornia, A.; Magnani, A.; Sessoli, R. Tetrairon(III) Single-Molecule Magnet Monolayers on Gold: Insights from ToF-SIMS and Isotopic Labeling. *Langmuir* **2014**, *30*, 8645–8649. [CrossRef]

23. Zhang, X.; Mu, S.; Chastanet, G.; Daro, N.; Palamarciuc, T.; Rosa, P.; Létard, J.-F.; Liu, J.; Sterbinsky, G.E.; Arena, D.A.; et al. Complexities in the Molecular Spin Crossover Transition. *J. Phys. Chem. C* **2015**, *119*, 16293–16302. [CrossRef]

24. Atzori, M.; Poggini, L.; Squillantini, L.; Cortigiani, B.; Gonidec, M.; Bencok, P.; Sessoli, R.; Mannini, M. Thermal and light-induced spin transition in a nanometric film of a new high-vacuum processable spin crossover complex. *J. Mater. Chem. C* **2018**, *6*, 8885–8889. [CrossRef]

25. Chandesris, D.; Lecante, J.; Petroff, Y. Two-electron resonances in transition metals. *Phys. Rev. B* **1983**, *27*, 2630–2635. [CrossRef]

26. Beniwal, S.; Zhang, X.; Mu, S.; Naim, A.; Rosa, P.; Chastanet, G.; Létard, J.-F.; Liu, J.; Sterbinsky, G.E.; Arena, D.A.; et al. Surface-induced spin state locking of the [Fe(H$_2$B(pz)2)$_2$(bipy)] spin crossover complex. *J. Phys. Condens. Matter* **2016**, *28*, 206002. [CrossRef]

27. Gupta, R.P.; Sen, S.K. Calculation of multiplet structure of core p-vacancy levels. II. *Phys. Rev. B* **1975**, *12*, 15. [CrossRef]

28. Ellingsworth, E.C.; Turner, B.; Szulczewski, G. Thermal conversion of [Fe(phen)$_3$](SCN)$_2$ thin films into the spin crossover complex Fe(phen)$_2$(NCS)$_2$. *RSC Adv.* **2013**, *3*, 3745. [CrossRef]

29. Zhang, X.; Palamarciuc, T.; Rosa, P.; Létard, J.-F.O.L.; Doudin, B.; Zhang, Z.; Wang, J.; Dowben, P.A. Electronic Structure of a Spin Crossover Molecular Adsorbate. *J. Phys. Chem.* **2012**, *116*, 23291–23296. [CrossRef]

30. Singhbabu, Y.N.; Kumari, P.; Parida, S.; Sahu, R.K. Conversion of pyrazoline to pyrazole in hydrazine treated N-substituted reduced graphene oxide films obtained by ion bombardment and their electrical properties. *Carbon N. Y.* **2014**, *74*, 32–43. [CrossRef]

31. Deleuze, M.S. Valence one-electron and shake-up ionization bands of polycyclic aromatic hydrocarbons. II. Azulene, phenanthrene, pyrene, chrysene, triphenylene, and perylene. *J. Chem. Phys.* **2002**, *116*, 7012–7026. [CrossRef]

32. Gengenbach, T.R.; Major, G.H.; Linford, M.R.; Easton, C.D. Practical guides for X-ray photoelectron spectroscopy (XPS): Interpreting the carbon 1s spectrum. *J. Vac. Sci. Technol. A* **2021**, *39*, 13204. [CrossRef]

33. Gruber, M.; Berndt, R. Spin-Crossover Complexes in Direct Contact with Surfaces. *Magnetochemistry* **2020**, *6*, 35. [CrossRef]

34. Kipgen, L.; Bernien, M.; Ossinger, S.; Nickel, F.; Britton, A.J.; Arruda, L.M.; Naggert, H.; Luo, C.; Lotze, C.; Ryll, H.; et al. Evolution of cooperativity in the spin transition of an iron(II) complex on a graphite surface. *Nat. Commun.* **2018**, *9*, 2984. [CrossRef]

35. Poneti, G.; Poggini, L.; Mannini, M.; Cortigiani, B.; Sorace, L.; Otero, E.; Sainctavit, P.; Magnani, A.; Sessoli, R.; Dei, A. Thermal and optical control of electronic states in a single layer of switchable paramagnetic molecules. *Chem. Sci.* **2015**, *6*, 2268–2274. [CrossRef]

36. Ossinger, S.; Näther, C.; Buchholz, A.; Schmidtmann, M.; Mangelsen, S.; Beckhaus, R.; Plass, W.; Tuczek, F. Spin Transition of an Iron(II) Organoborate Complex in Different Polymorphs and in Vacuum-Deposited Thin Films: Influence of Cooperativity. *Inorg. Chem.* **2020**, *59*, 7966–7979. [CrossRef]

37. Warner, B.; Oberg, J.C.; Gill, T.G.; El Hallak, F.; Hirjibehedin, C.F.; Serri, M.; Heutz, S.; Arrio, M.-A.; Sainctavit, P.; Mannini, M.; et al. Temperature- and Light-Induced Spin Crossover Observed by X-ray Spectroscopy on Isolated Fe(II) Complexes on Gold. *J. Phys. Chem. Lett.* **2013**, *4*, 1546–1552. [CrossRef] [PubMed]

38. Miyamachi, T.; Gruber, M.; Davesne, V.; Bowen, M.; Boukari, S.; Joly, L.; Scheurer, F.; Rogez, G.; Yamada, T.K.; Ohresser, P.; et al. Robust spin crossover and memristance across a single molecule. *Nat. Commun.* **2012**, *3*, 938. [CrossRef] [PubMed]

39. Serrano, G.; Poggini, L.; Briganti, M.; Sorrentino, A.L.; Cucinotta, G.; Malavolti, L.; Cortigiani, B.; Otero, E.; Sainctavit, P.; Loth, S.; et al. Quantum dynamics of a single molecule magnet on superconducting Pb(111). *Nat. Mater.* **2020**, *19*, 546–551. [CrossRef]

40. Gopakumar, T.G.; Bernien, M.; Naggert, H.; Matino, F.; Hermanns, C.F.; Bannwarth, A.; Mühlenberend, S.; Krüger, A.; Krüger, D.; Nickel, F.; et al. Spin-Crossover Complex on Au(111): Structural and Electronic Differences between Mono- and Multilayers. *Chem.—Eur. J.* **2013**, *19*, 15702–15709. [CrossRef] [PubMed]

41. Dishner, M.H.; Ivey, M.M.; Gorer, S.; Hemminger, J.C.; Feher, F.J. Preparation of gold thin films by epitaxial growth on mica and the effect of flame annealing. *J. Vac. Sci. Technol. A Vac. Surf. Film.* **1998**, *16*, 3295–3300. [CrossRef]

42. Ohresser, P.; Otero, E.; Choueikani, F.; Chen, K.; Stanescu, S.; Deschamps, F.; Moreno, T.; Polack, F.; Lagarde, B.; Daguerre, J.-P.; et al. DEIMOS: A beamline dedicated to dichroism measurements in the 350–2500 eV energy range. *Rev. Sci. Instrum.* **2014**, *85*, 013106. [CrossRef]

43. Henke, B.L.; Liesegang, J.; Smith, S.D. Soft-x-ray-induced secondary-electron emission from semiconductors and insulators: Models and measurements. *Phys. Rev. B* **1979**, *19*, 3004–3021. [CrossRef]

44. Heinrich, A.J.; Oliver, W.D.; Vandersypen, L.M.K.; Ardavan, A.; Sessoli, R.; Loss, D.; Jayich, A.B.; Fernandez-Rossier, J.; Laucht, A.; Morello, A. Quantum-coherent nanoscience. *Nat. Nanotechnol.* **2021**, *16*, 1318–1329. [CrossRef] [PubMed]